

Solution to EDGES anomaly with a millicharge of possible string origin

SUSY2022

University of Ioannina, Greece

June 27- July 2, 2022

PN

Northeastern University, Boston

July 1, 2022

Outline

- Thermal history of the universe in brief. Physics of 21 cm line at cosmic dawn.
- Data from “**The Experiment to Detect the Global Epoch of Reionization Signature (EDGES)**”
- Theoretical analysis: Stueckelberg hidden sector model with milli-charge dark matter.
 - Early times: High redshift
 - Late times: Low redshift
- Connection with strings. Future prospects¹

¹Based on: A. Aboubrahim, PN and Z. Y. Wang, JHEP **12**, 148 (2021).

Thermal history of the universe in brief

Time	Temp	$z = \lambda_{\text{obs}}/\lambda_{\text{rest}} - 1$	Epoch
10^{-43}s	10^{19} GeV		Quantum gravity: $E\sqrt{G_N} = 1$
10^{-37}s	10^{16} GeV		SUGRA/grand unification ²
10^{-12}s	10^3 GeV		Weak scale supersymmetry ³
10^{-10}s	10^2 GeV		Higgs & EW phase transition ⁴
$10^{-4.5}\text{s}$	0.2 GeV		Quarks to hadrons transition ⁶
(1-100) s	(1 – 0.1) MeV		BBN ($^2\text{H}, ^3\text{H}, ^4\text{He}, ^7\text{Li}$)
380,000 yr	~ 1 eV	1100 (recombination)	$e^- + p \rightarrow H(1s) + \gamma$, CMBR
<u>(0.5-1) billion yr</u>	<u>$\sim 10^{-3}$ eV</u>	<u>(10 – 30)</u>	<u>Reionization-cosmic dawn.</u>
13.8 billion yr	2.35×10^{-4} eV	$z = 0$	Current times

² $SO(10) \rightarrow SU(3) \times SU(2) \times U(1)_Y$

³ Charginos, sleptons and squarks with masses in TeV range expected and discoverable at LHC.

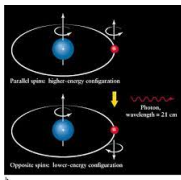
⁴ $SU(2) \times U(1)_Y \rightarrow \text{weak force} + \text{Electromagnetism}$.

⁵ Higgs breaking: $SU(2) \times U(1) \rightarrow U(1)_{\text{em}}$.

⁶ Quarks and gluons become bound into protons and neutrons.

21 cm line at cosmic dawn

- 21-cm line arises from the spin transition from the triplet state to the singlet state and vice-versa in the ground state of neutral hydrogen.



- Spin temperature T_s is defined by the relative abundance of triplet vs singlet states of the Hydrogen gas⁷

$$\frac{n_1}{n_0} = 3e^{-\frac{T_*}{T_s}},$$

where 3 is the ratio of the spin degrees of freedom for the triplet versus the singlet state, T_* is defined by $\Delta E = kT_*$, where $\Delta E = 1420$ MHz is the energy difference at rest between the two spin states,

$$T_* \equiv \frac{hc}{k\lambda_{21\text{cm}}} = 0.068\text{K}.$$

⁷ Baryon temperature $T_B = T_s$

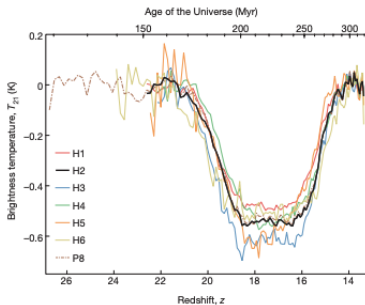
EDGES data

EDGES reported an absorption profile centered at the frequency $\nu = 78$ MHz in the sky-averaged spectrum. The quantity of interest is the brightness temperature T_{21} of the 21-cm line defined by

$$T_{21}(z) = \frac{T_s - T_\gamma}{1 + z} (1 - e^{-\tau}),$$

τ is the optical depth for the transition.

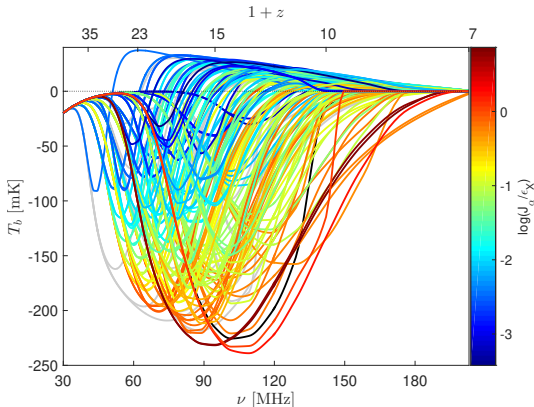
The analysis of Bowman et al⁸ finds that at $z \sim 17$, $T_{21} = -500^{+200}_{-500}$ mK at 99% C.L.



⁸J. D. Bowman, A. E. E. Rogers, R. A. Monsalve, T. J. Mozdzen and N. Mahesh, *Nature* **555**, no.7694, 67-70 (2018).

- Cohen et. al.⁹ analyzed the 21-cm signal as a function of the redshift and found that using 193 models within in the standard cosmology the temperature T_{21} is maximally

$$T_{21} \simeq -250 \text{ mK}, \quad z = (6 - 40).$$



The color indicates the ratio between the $\text{Ly}\alpha$ intensity (in units of $\text{erg s}^{-1} \text{ cm}^{-2} \text{ Hz}^{-1} \text{ sr}^{-1}$) and the X-ray heating rate (in units of $\text{eV s}^{-1} \text{ baryon}^{-1}$) at the minimum point.

⁹A. Cohen, A. Fialkov, R. Barkana and M. Lotem, Mon. Not. Roy. Astron. Soc. **472**, no.2, 1915-1931 (2017) [arXiv:1609.02312 [astro-ph.CO]].

Possible explanations of EDGES anomaly

- Astrophysical phenomena such as radiation from stars and star remnants.
- The CMB background radiation temperature is hotter than expected.
- **The baryons are cooler than what Λ CDM predicts. ✓**
- Modification of cosmological evolution: inclusion of dark energy such as Chaplin gas.

These are a large number of authors involved in these works ¹⁰

- I will discuss here the baryon cooling by millicharge DM which assumes a small percentage of DM ($\sim 0.3\%$) is millicharged and baryons become cooler by Rutherford scattering from colder dark matter.
- **However, before going further one might ask what the origin of millicharge is.**

¹⁰Barkana, Loeb, Prichard, Furlanetto, Kovetz, Munoz, Dvorkin, H Liu, Moroi, Kamiokonski, Valentino, Vagnozzi

Millicharge with two $U(1)$'s: $U(1)_X$ and $U(1)_Y$

- Holdom showed that with kinetic mixing, massless gauge fields of two $U(1)$'s allow a millicharge¹¹ which, however, is phenomenologically not viable.
- The problem of two massless gauge bosons is overcome in Stueckelberg mass mixing of two $U(1)$ gauge fields allows a millicharge with one massless gauge field¹².

$$\begin{aligned}\mathcal{L} &= \mathcal{L}_{\text{SM}} + \mathcal{L}_{\text{hid}} + \mathcal{L}_{\text{SM-hid}}, \\ \mathcal{L}_{\text{hid}} &= -\frac{1}{4}C_{\mu\nu}C^{\mu\nu} + i\bar{D}\gamma^\mu\partial_\mu D - m_D\bar{D}D - \frac{1}{2}(\partial_\mu\phi\partial^\mu\phi) \\ &\quad + g_X Q_X \bar{D}\gamma^\mu D C_\mu + \lambda D\bar{D}\phi. \\ \mathcal{L}_{\text{SM-hid}} &= -\frac{1}{2}(\partial_\mu\sigma + M_1 C_\mu + M_2 B_\mu)^2,\end{aligned}$$

Particles : D, ϕ , (dark fermion, dark scalar).

: C_μ, σ , (dark gauge field, dark axion).

M_1, M_2 , (Stueckelberg masses).

$\epsilon = M_2/M_1$, (millicharge= $e\epsilon$).

¹¹B. Holdom, Phys. Lett. B 166 (1986) 196.

¹²B. Kors and PN., Phys. Lett. B **586**, 366-372 (2004); JHEP **12**, 005 (2004);
A. Aboubrahim, PN, Z. Y. Wang, JHEP **12**, 148 (2021)

- Couplings of dark photon and of dark fermion in St model:

$$\begin{aligned}
 L_D = & \epsilon_\gamma^D e \bar{D} \gamma^\mu D A_\mu^\gamma \\
 & + \epsilon_Z^D e \bar{D} \gamma^\mu D Z_\mu \\
 & + \epsilon_f \bar{f} \gamma^\mu (v'_f - \gamma_5 a'_f) f A_\mu^{\gamma'} \\
 & + g_X \bar{D} \gamma^\mu D A_\mu^{\gamma'}
 \end{aligned}$$

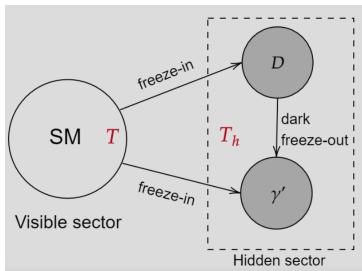
where $\epsilon_\gamma^D, \epsilon_Z^D, \epsilon_f$ are $O(\epsilon = M_2/M_1)$ and $g_X = O(1)$.

- In addition to the millicharge $\epsilon_\gamma^D e$, all of the remaining couplings are needed for generating a consistent cosmology.

Early time evolution.

The early time evolution determines the boundary conditions for late time evolution specifically the amount of millicharge dark matter.

Hidden and visible sectors in different heat baths



A consistent analysis involves an equation for the thermal evolution function $\xi = T_h/T$.

Thermal evolution of the universe with different different heat baths

- In most treatments separate entropy conservation for hidden and visible entropies is assumed. However, for coupled visible and hidden sectors only the total entropy is conserved.

$$\frac{d(a^3 s_v)}{dt} = 0, \frac{d(a^3 s_h)}{dt} = 0 \quad (\text{invalid}).$$
$$\frac{d(a^3 s)}{dt} = 0, \quad s = s_v + s_h. \quad \checkmark$$

- The total entropy density and the Hubble parameter involve two temperatures: T, T_h .

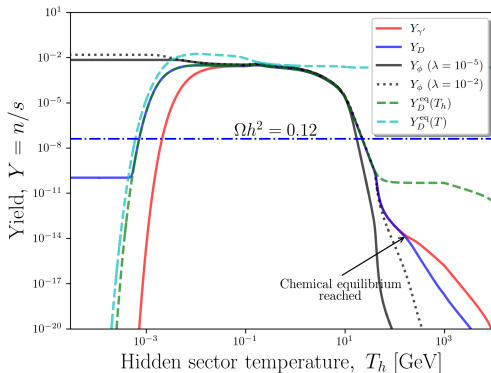
$$s = \frac{2\pi^2}{45} (h_{\text{eff}}^h T_h^3 + h_{\text{eff}}^v T^3), \quad H^2 = \frac{8\pi G_N}{3} (\rho_v(T) + \rho_h(T_h)).$$

- Thermal evolution with two heat baths involves evolution equation for $d\xi/dT_h$. Recently a general analysis on the thermal evolution of the universe with different heat baths has been developed ¹³.
- We use this formalism in the analysis of the relic density of the millicharged dark matter.

¹³ A. Aboubrahim, W. Z. Feng, P.N. and Z. Y. Wang, Phys. Rev. D **103**, no.7, 075014 (2021) ([2 heat baths](#)); JHEP **06**, 086 (2021) ([3 heat baths](#))
A. Aboubrahim and P. N., [arXiv:2205.07316 [hep-ph]] ([n heat baths](#)).

Relic density of millicharged dark matter

Dark freezeout: Chemical decoupling of dark fermions from dark photons ¹⁴



¹⁴ A. Aboubrahim, PN and Z. Y. Wang, JHEP **12**, 148 (2021).

Late time evolution

Evolution of temperature of baryons (T_B) and of DM (T_D) at Reionization

For the Stueckelberg extended model the evolution equations of baryon and DM temperatures, T_B and T_D , and of the ionization rate x_e are given by ¹⁵

$$\begin{aligned}(1+z) \frac{dT_D}{dz} &= 2T_D + \frac{\Gamma_\phi}{H(z)} (T_D - T_\phi) - \frac{2}{3H(z)} \dot{Q}_D, \\(1+z) \frac{dT_B}{dz} &= 2T_B + \frac{\Gamma_c}{H(z)} (T_B - T_\gamma) - \frac{2}{3H(z)} \dot{Q}_B, \\H(z)(1+z) \frac{dx_e}{dz} &= C \left[n_H \alpha_B x_e^2 - 4(1-x_e) \beta_B e^{-3E_0/4T_\gamma} \right], \\H(z) &= H_0 \sqrt{\Omega_m (1+z)^3 + \Omega_\Lambda + \Omega_k (1+z)^2}.\end{aligned}$$

$$\Omega_m = \Omega_B + \Omega_c, \Omega_\Lambda = 0.685, \Omega_k = 0.001.$$

C is Peebles factor, Γ_c is the Compton interaction rate; Γ_ϕ (negligible).

\dot{Q}_B, \dot{Q}_D couple T_B and T_D via millicharge couplings.

α_B is a recombination co-efficient and β_B is photoionization rate.

¹⁵ A. Aboubrahim, PN and Z. Y. Wang, JHEP **12**, 148 (2021). For earlier work see J. B. Muñoz and A. Loeb, Nature **557**, no.7707, 684 (2018). E. D. Kovetz, V. Poulin, V. Gluscevic, K. K. Boddy, R. Barkana and M. Kamionkowski, Phys. Rev. D **98**, no.10, 103529 (2018)

Peebles factor C^{16}

$$C = \frac{\frac{3}{4}R_{\text{Ly}\alpha} + \frac{1}{4}\Lambda_{2s,1s}}{\beta_B + \frac{3}{4}R_{\text{Ly}\alpha} + \frac{1}{4}\Lambda_{2s,1s}}.$$

- $R_{\text{Ly}\alpha}$: Rate of escape of Lyman alpha $\text{Ly}\alpha$ photons

$$R_{\text{Ly}\alpha} = \frac{8\pi H(z)}{3n_{\text{H}}x_{1s}\lambda_{\text{Ly}\alpha}^3}.$$

- $\lambda_{\text{Ly}\alpha} = 2\pi/E_{n1}$; $E_{n1} = E_2 - E_0 = 3/4E_0$.
- $\Lambda_{2s,1s} = 8.22 \text{ s}^{-1}$: The total $2s \rightarrow 1s$ two-photon decay rate.
- $n_{\text{H}}x_{1s} \approx 1 - x_e$: Number density of ground state population of neutral hydrogen in the recombination epoch.

¹⁶P. J. E. Peebles, *Astrophys. J.* **153**, 1 (1968).

Compton interaction rate Γ_c

$$\Gamma_c = \frac{64\pi^3\alpha^2 T_\gamma^4}{135m_e^3} \frac{x_e}{1 + x_e + f_{\text{He}}}.$$

- T_γ : CMB photon temperature

$$T_\gamma = 2.726(1 + z).$$

- α : Fine structure constant.
- f_{He} : Helium fraction.

α_B and β_B

- α_B is a recombination co-efficient given by

$$\alpha_B(T_B) = 10^{-13} \frac{a(10^{-4}T_B)^b}{1 + c(10^{-4}T_B)^d},$$

where $a = 4.309$, $b = -0.6166$, $c = 0.6703$, and $d = 0.5300$.

- β_B is photoionization rate which can be obtained from α_B by detailed balance

$$\beta_B(T_\gamma) = \frac{g_e}{4} e^{E_2/T_\gamma} n_H \alpha_B(T_B = T_\gamma),$$

$$g_e = \left(\frac{\mu_e T_\gamma}{2\pi} \right)^{3/2} \frac{1}{n_H},$$

and $\mu_e = m_e m_p / (m_e + m_p)$.

The brightness temperature of the 21-cm line

The quantity of interest in explaining the EDGES result is the brightness temperature T_{21} of the 21-cm line defined by

$$T_{21}(z) = \frac{T_s - T_\gamma}{1 + z} (1 - e^{-\tau}),$$

τ is the optical depth for the transition

$$\tau = \frac{3T_* A_{10} \lambda_{21}^3 n_{\text{HI}}}{32\pi T_s H(z)}.$$

Here

$$T_* = 0.068\text{K}$$

$$A_{10} = 2.869 \times 10^{-15} \text{ s}^{-1} \quad \text{Einstein co-efficient for spontaneous hyperfine transition}$$

$$\lambda_{21} = 21.1\text{cm}$$

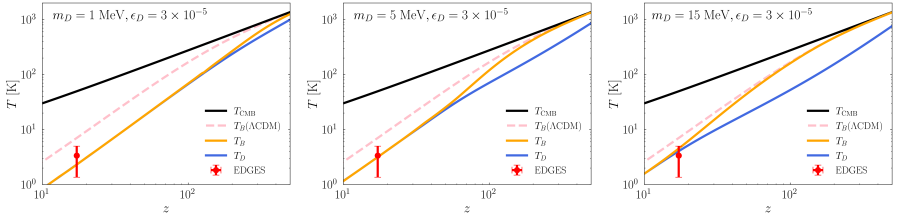
$$n_{\text{HI}} = n_{\text{H}}(1 - x_e),$$

x_e : free electron fraction.

$$T_s = T_B$$

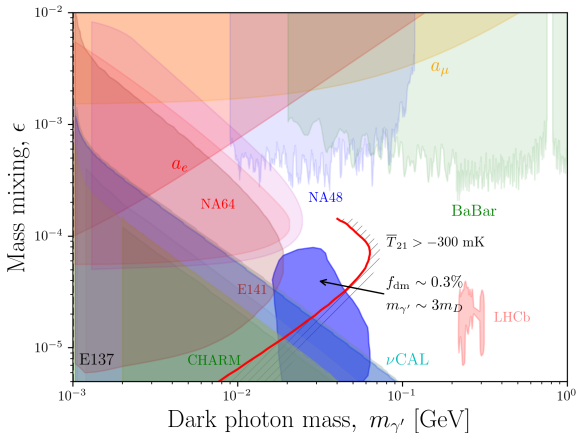
$H(z)$: Hubble at redshift z

Fit to EDGES data ¹⁷



The evolution of the CMB (black line), baryons (orange line), and DM (blue line) as a function of the redshift. The pink dashed line is the T_B evolution in the ΛCDM model. The three panels correspond to three different values of m_D and fixed $\epsilon_D = 3 \times 10^{-5}$ and $f_{\text{dm}} = 0.3\%$. It is seen that for m_D small, baryons and DM have a faster heat exchange so they thermalize early on and DM cools baryons more efficiently. The red point with vertical error bars in each of the three panels represents the EDGES measurement.

¹⁷ A. Aboubrahim, PN and Z. Y. Wang, JHEP **12**, 148 (2021).



Plot of the mass mixing parameter ϵ versus the dark photon mass where the constraints shown from various experiments are discussed in the text. The region in blue corresponds to the parameter space giving $f_{\text{dm}} \sim 0.3\%$ and is consistent with the allowed region in the ϵ - m_D plane only within the region not excluded by \bar{T}_{21} bounded by the hatched red curve. Here we set $Q_X = 1$ and $g_X = 0.2$. $m_{\gamma'} \sim 3m_D$ indicates that we are able to deplete the DM relic density to the required fraction.¹⁸

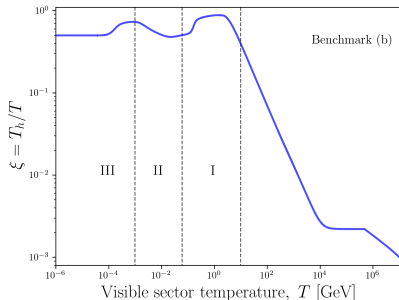
¹⁸ A. Aboubrahim, PN and Z. Y. Wang, JHEP **12**, 148 (2021).

$$\Delta N_{eff}$$

The extra relativistic degrees of freedom: one has

$$\Delta N_{eff} \simeq \frac{4\Delta n_b}{7} \left(\frac{11}{4} \right)^{4/3} \left(\frac{T_h}{T} \right)^4$$

In the model $\Delta n_b = 1$ for the massless field ϕ . At BBN time $\xi = T_h/T = 0.5$ which gives¹⁹ $\Delta N_{eff} \sim 0.14$ consistent with the experimental limit of $\Delta N_{eff} \sim 0.2$.



Evolution of $\xi = T_h/T$ as a function of the visible sector temperature T . The ratio levels off at $\xi = 0.5$.

¹⁹A. Aboubrahim, PN and Z. Y. Wang, JHEP **12**, 148 (2021).

Millicharges, BSM physics, quantum gravity

Millicharges do not exist in the Standard Model. However, they can arise in BSM physics. Some examples:

- Witten effect: In CP non-conserving theories, the electric charge of a t' Hooft-Polyakov magnetic monopole will be $-e\theta/2\pi$ which is a millicharge if θ is small²⁰.
- Kinetic mixing of two $U(1)$'s can generate a millicharge when both gauge bosons are massless²¹. The millicharge disappears if one of the gauge boson becomes massive such as for the case of a massive dark photon²².
- As noted earlier perhaps the simplest way to degenerate a millicharge when there is one massless gauge field is via mass mixing in the Stueckelberg mechanism²³. St mechanism has a strong link with strings²⁴.
- Banks and Seiberg point out²⁵ that quantum gravity puts a constraint on the mixing parameter in that a single massless field coupling to charged matter requires the charge to be rational.

²⁰E. Witten, Phys. Lett. B86, 283-287 (1979).

S. Coleman, "Magnetic monopole fifty years later", A. Zichichi (ed.) Plenum 817p.

²¹B. Holdom, Phys. Lett. B 166 (1986) 196.

²²D. Feldman, Z. Liu and P. N., Phys. Rev. D 75, 115001 (2007).

²³B. Kors and P.N., Phys. Lett. B **586**, 366-372 (2004).

²⁴For $U(1)$'s in strings see, e.g., Abel, Benakli, Feng, Ibanez, Ignatios, Kiritsis, Rizos, Shiu, . . .

²⁵T. Banks and N. Seiberg, Phys. Rev. D **83**, 084019 (2011).

Stueckelberg mechanism from strings

- Green-Schwarz ²⁶ found that in the low energy limit of Type I strings the kinetic energy of 2-tensor B_{MN} of 10D SUGRA gives

$$\partial_{[P}B_{MN]} \rightarrow \partial_{[P}B_{MN]} + \omega_{PMN}^{(Y)} - \omega_{PMN}^{(L)}$$

Subsequent to GS work the low energy $N = 1$ supergravity Lagrangian in 10D coupled to Yang-Mills was generalized fully to order κ^2 ($\kappa = M_{\text{Pl}}^{-1}$) ²⁷.

- Expanding the kinetic term for B_{MN} one has from the Yang-Mills Chern-Simons form

$$\partial_{[P}B_{MN]} + A_{[P}F_{MN]} + \cdots$$

Dimensional reduction to 4D with a vacuum expectation value for the internal gauge field strength, $\langle F_{ij} \rangle \neq 0$, leads to

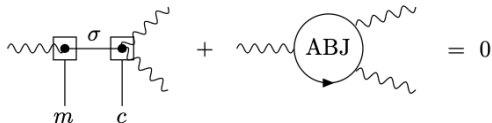
$$\partial_\mu B_{ij} + A_\mu F_{ij} + \cdots \sim \partial_\mu \sigma + m A_\mu,$$

on identifying the internal components B_{ij} with the pseudo-scalar σ and the value of the gauge field strength with the mass parameter m . Thus A_μ and σ have a Stueckelberg coupling of the form $A_\mu \partial^\mu \sigma$.

²⁶ M. B. Green and J. H. Schwarz, Phys. Lett. 149, 117(1983)

²⁷ A. Chamseddine, PN, PRD 34, 12, 3769 (1986);
E. Bergshoeff, A. Salam and E. Sezgin, Nucl. Phys. B **279**, 659-683 (1987);
L.J. Romans and N.P. Warner, Nucl. Phys. 8273, 320 (1986).

The Stueckelberg mechanism enters in the Green-Schwarz anomaly cancellation where the ABJ loop contribution to the anomaly is cancelled by a tree contribution.



The tree contribution arises here from the exchange of the σ field.

$$mA^\mu \partial_\mu \sigma + \frac{c\sigma}{m} \text{Tr}(F \wedge F)$$

An anomalous $U(1)$ will get massive through the Stueckelberg mechanism since $m.c \neq 0$, but a non-anomalous $U(1)$ will do so as well if $c = 0$ but $m \neq 0$.

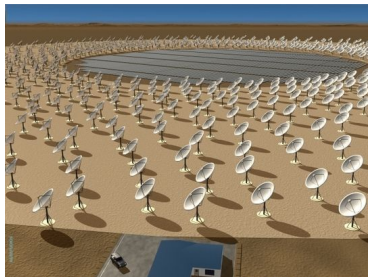
Strings could thus be the embedding framework for Stueckelberg mechanism and for millicharge.

Future prospects to probe 21 cm line at Cosmic Dawn

- The Low Frequency Array (**LOFAR**) in Netherlands. Bandwidth: (10-230)MHz.
- The Murchison Widefield Array (**MWA**) in Western Australia. (80-300) MHz.
- Broadband Instrument for the Global HydrOgen Reionization Signal (**BIGHORNS**) Murchison Radio-astronomy Observatory. (70-300)MHz.
- Large-aperture Experiment to Detect the Dark Ages (**LEDA**). Owen's valley, California; Socorro, New Mexico. (30-88)MHz.
- The Precision Array to Probe the Epoch of Reionization (**PAPER**), Northern Cape, South Africa. (100-200) MHz
- the Hydrogen Epoch of Reionization Array (**HERA**) in South Africa. (50- 250) MHz.
- The Square Kilometer Array (**SKA**) in southern hemisphere with cores in South Africa and Australia with headquarters at Jodrell Bank Observatory in UK. (70 MHz-25 GHz).

Conclusion

- A variety of current and future telescopes will probe the cosmic dawn in greater depth and will test the EDGES result.
- If the EDGES effect is confirmed and millicharge turns out to be the preferred solution, it would require a paradigm shift in our view of the standard model of particle physics as well as the standard cosmological Λ CDM model.
- Quantum gravity may turn out to be the right framework where to embed the millicharge.



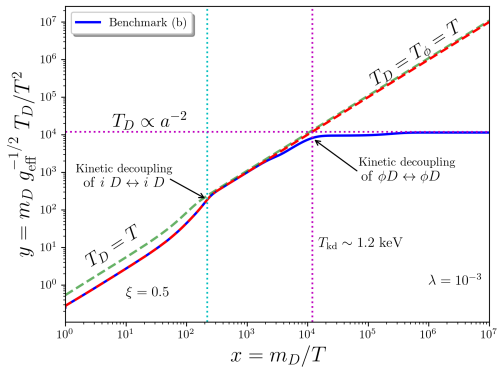
SKA MeerKAT, South Africa. SKA Murchinson, Australia.
70 MHz-25 GHz.



Large Aperture Experiment to Detect the Dark Ages (LEDA) at Owens Valley in California. (30-88) MHz.

Extra slides

Kinetic equilibrium



The sources \dot{Q}_B and \dot{Q}_D

The quantities \dot{Q}_B and \dot{Q}_D couple the evolution of T_B and T_D and are

$$\dot{Q}_B = f_{\text{dm}} \frac{\rho_D}{m_D} \frac{x_e}{1 + f_{\text{He}}} \sum_{t=e,p} \frac{m_D m_t}{(m_D + m_t)^2} \frac{\sigma_0}{\bar{u}_t} \left[\sqrt{\frac{2}{\pi}} \frac{e^{-r_t^2/2}}{\bar{u}_t^2} (T_D - T_B) + m_D \frac{F(r_t)}{r_t} \right], \quad (1)$$

$$\dot{Q}_D = n_{\text{H}} x_e \sum_{t=e,p} \frac{m_D m_t}{(m_D + m_t)^2} \frac{\sigma_0}{\bar{u}_t} \left[\sqrt{\frac{2}{\pi}} \frac{e^{-r_t^2/2}}{\bar{u}_t^2} (T_B - T_D) + m_t \frac{F(r_t)}{r_t} \right], \quad (2)$$

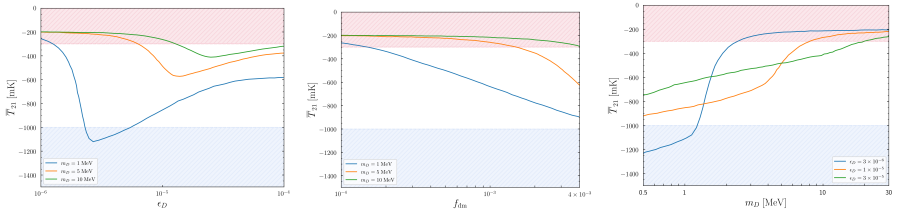
$f_{\text{He}} \equiv n_{\text{He}}/n_{\text{H}} \approx 0.08$ is the ratio of the helium to hydrogen number densities. The function $F(r_t)$ is given by

$$F(r_t) \equiv \text{Erf} \left(\frac{r_t}{\sqrt{2}} \right) - \sqrt{\frac{2}{\pi}} r_t e^{-r_t^2/2}. \quad (3)$$

Here $r_t \equiv V_{DB}/\bar{u}_t$, where \bar{u}_t is the average velocity due the thermal motion defined by

$$\bar{u}_t = \sqrt{T_B/m_t + T_D/m_D}. \quad (4)$$

m_t is the target mass which could be either an electron or a proton.



Exhibition of the dependence of \bar{T}_{21} at $z = 17.2$ on ϵ_D (left panel), on f_{dm} (middle panel) and on m_D (right panel). Left panel: the three curves correspond to $m_D = 1$ MeV (blue line), 5 MeV (orange line) and 10 MeV (green line) with a fixed $f_{dm} = 0.3\%$. Middle panel: The three curves correspond to the same three values of m_D as in the left panel except that here ϵ_D is fixed at $\epsilon_D = 10^{-5}$. Right panel: Here the three curves correspond to values of ϵ_D to be 3×10^{-6} (blue line), 1×10^{-5} (orange line) and 3×10^{-5} (green line) with a fixed $f_{dm} = 0.3\%$. In all panels, the red hatched region is excluded by $\bar{T}_{21} > -300$ mK while the blue hatched region is excluded by $\bar{T}_{21} < -1000$ mK. ²⁸

²⁸ A. Aboubrahim, PN and Z. Y. Wang, JHEP **12**, 148 (2021).